Dynamic hole trapping in InAs/AlGaAs/InAs quantum dot molecules

Weiwen Liu,[1] Allan S. Bracker,[2] Daniel Gammon,[2] and Matthew F. Doty[1,*]

[1]*Department of Materials Science and Engineering, University of Delaware, Newark, Delaware 19716, USA*

[2]*Naval Research Laboratory, Washington, DC 20375, USA*

Charges and spins confined in quantum dots and quantum dot molecules are of great interest for new optoelectronic device applications. The strong confinement in quantum dot structures leads to unique interactions among electrons and holes. A detailed understanding of the magnitude and dynamics of these charge-carrier interactions will be essential to the development of future devices. We present experimental evidence of holes trapped in metastable higher-energy states of InAs/AlGaAs/InAs quantum dot molecules. We present a model for the kinetic pathways that lead to this dynamic hole trapping and analyze the consequences of dynamic hole trapping for carrier relaxation and optical emission.

PACS number(s): 78.20.Ls, 78.47.−p, 78.55.Cr, 78.67.Hc

I. INTRODUCTION

Quantum dots (QDs) and quantum dot molecules (QDMs) are attractive components for next generation optoelectronic devices because the discrete energy states and properties of confined charges can be engineered with structure and composition.[1–5] Because charges are strongly confined in both QDs and QDMs, there are significant many-body interactions in structures containing more than one electron or hole. These interactions introduce Coulomb shifts and spin fine structure.[6–9] In InAs/GaAs QDMs consisting of two QDs stacked along the growth direction there are multiple spatial configurations for a given number of confined electrons and holes.[6,10,11] The magnitude of Coulomb and spin interactions in QDMs depends on the number and spatial configuration of charges.[12–14] Coherent tunneling of charges between the spatial configurations leads to new molecular energy eigenstates and new physical processes that can be controlled by applied electric fields.[15–17]

The charge-carrier interactions in both QDs and QDMs lead to complex energy shifts and new dynamics that provide both challenges and opportunities for new devices. Spin precession and quantum control, for example, require minimal fluctuations in energy in order to avoid dephasing and decoherence.[18–21] On the other hand, Coulomb energy shifts in the presence of optically generated electrons or holes provide a powerful new tool for optical control, including coherent spin rotations. We present experimental measurements of a single QDM in which one extra hole can be trapped in a metastable higher-energy state of the QDM. We present a model for the kinetic pathways which lead to this dynamic hole trapping and then analyze the impact of this dynamically trapped hole on carrier relaxation and Coulomb interactions. Our model provides insight into effects that must be managed in the development of future devices.

II. SAMPLE AND EXPERIMENT

InAs/GaAs QDMs studied in recent years frequently utilize intentional asymmetries in the size of the two QDs to controllably achieve coupling of electrons or holes within a certain range of net electric fields.[17] For example, a QDM grown on an *n*-type substrate and designed for coherent tunneling of electrons utilizes a bottom QD truncated to a shorter height than the top QD [see Fig. 1(b)]. A natural consequence of this asymmetry is that the hole levels for such a QDM are significantly offset in energy, inducing the holes to relax to the lower energy hole state located in the top QD [Fig. 1(b)]. We recently designed, fabricated, and tested a QDM containing an AlGaAs barrier between the two QDs. The AlGaAs was added to controllably create a tunable *g* factor for a single electron confined in a molecular state of the QDM.[5,15] In this paper we show that the inclusion of this AlGaAs barrier can inhibit hole relaxation leading to a single hole trapped in the higher-energy state of the bottom QD. We show that the hole trapping occurs with a probability determined by competing charge relaxation and tunneling dynamics.

The QDM studied here is grown by molecular beam epitaxy (MBE) and consists of two InAs QDs separated by an AlGaAs barrier (see Fig. 1). The top QD nucleates above the bottom QD because of the strain introduced by the bottom QD. The individual heights of the two QDs are controlled by the In-flush technique. The 9-nm barrier between the QDs consists of 3 nm of $Al_{0.3}Ga_{0.7}As$ sandwiched between two 3-nm layers of GaAs. The dot is embedded in an *n*-type Schottky diode structure so that the relative energy levels of the two QDs can be precisely controlled with applied electric field. The applied electric field also controls the total charge occupancy of the QDM as the confined energy levels are tuned relative to the Fermi level set by the doped substrate. The top contact is made with a thin layer of titanium capped by an aluminum shadow mask containing 1-μm apertures defined by *e*-beam lithography. These apertures allow us to perform optical spectroscopy on individual QDMs.

Individual QDMs are excited with a continuous wave diode laser at 895 nm. The photoluminescence (PL) emitted by the QDM is collected by a high numerical aperture lens, dispersed by an 0.75-m spectrometer that has an 1100 groove/mm grating, and detected with a liquid-nitrogen-cooled charge-coupled diode (CCD). We present results from a single QDM in which the discrete PL lines can be assigned to specific charge configurations. This QDM is representative of the six we have studied experimentally. The energies of the detected PL lines are plotted in Fig. 2 as a function of the net electric field. Indirect PL transitions that involve an electron and hole in separate QDs have significantly different intensities than
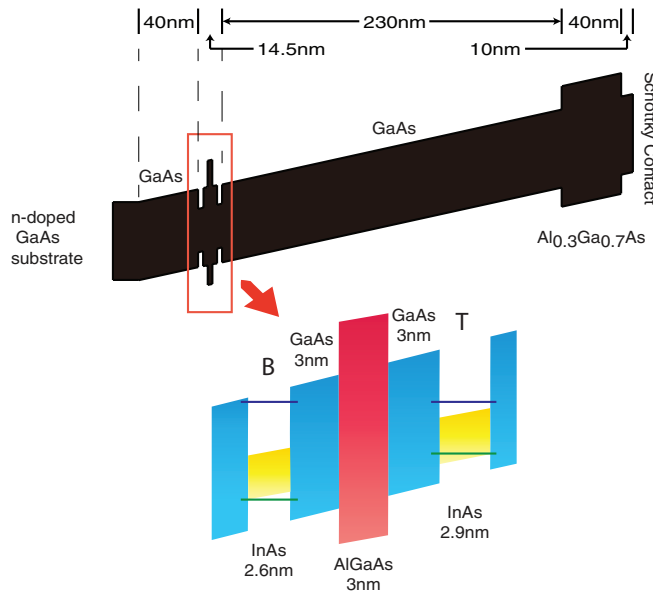
FIG. 1. (Color online) (a) Schematic band diagram of the QDM sample. (b) Detailed schematic of QDM composition and size and lowest confined energy levels for electrons and holes in the two QDs of the QDM.

direct transitions involving electrons and holes in the same QD. Consequently, Fig. 2 presents only the energy, and not the intensity, of the observed PL lines. The data are acquired with relatively long integration times, allowing us to see multiple spectral lines arising from a variety of configurations of the number and spatial location of charges.

Most of the PL lines presented in Fig. 2 can be assigned to specific charge states using the characteristic anticrossing signatures and energy shifts.[5,11] All of the assigned PL lines originate in optical recombination involving a hole confined in the top QD. The black triangles originate in the neutral exciton state (X^0: one electron and one hole). The red diamonds

originate in the biexciton state (XX^0: two electrons and two holes). The blue squares originate in the doubly negatively charged trion state (X^{2-}: three electrons and one hole). The assignment of these PL lines to these charge states is based on several rules:

(1) The neutral exciton (X^0) has only a single anticrossing because electrons can tunnel in the optically excited state and there are no charge carriers in the optical ground state. The anticrossing of the X^0 state in Fig. 2 occurs at F_1.

(2) All charge configurations other than X^0 exhibit an x-shaped pattern as a result of anticrossings arising from coherent tunneling in both the optically excited and the optical ground states (i.e., before and after PL emission).[12]

(3) The final state of the biexciton (XX^0) PL emission is the initial state of the X^0. Consequently, one group of curving of the spectrums from the XX^0 state occurs at the same electric field as the neutral exciton anticrossing (e.g., F_1 in Fig. 2).

(4) The intensity of PL emitted from biexciton states increases more rapidly than the intensity of PL emitted from the X^0 state as the power of the exciting laser increases (data not shown).

(5) One of the X^{2-} charge configurations is similar in energy to the direct X^0 transition (e.g., approximately 1337.5 meV) because in both cases there is only one electron and one hole in the top QD.

(6) The other direct transition of the X^{2-} (approximately 1334.5 meV) has two electrons and one hole in the top QD and therefore is typically redshifted relative to the X^0 PL line by 3–6 meV.

(7) The anticrossing energy gap indicates the tunneling strength. For the X^{2-} state, the anticrossing gap at low electric field ($F_3 \sim 3$ kV/cm) should be $\sqrt{2}$ larger than the anticrossing gap at higher fields ($F_4 \sim 7$ kV/cm) because there are two electrons that can tunnel in the optical ground state and only one electron that can tunnel in the optically excited state.[5,11]

III. DYNAMIC HOLE TRAPPING

Although most of the observed PL lines can be explained by existing models, there are three important discrepancies. First, there are two groups of lines (open green circles, solid purple circles) that remain unexplained. These unexplained PL lines "echo" the X^0 and X^{2-} states, but are offset by 0.5–2 meV and are visible only in a limited range of electric fields. Second, the biexciton PL observed (red diamonds) does not have the energy structure typical of a QDM in which electrons tunnel and holes relax to the top QD. In the next sections we show that all of these new features are explained by the presence of a single "spectator" hole trapped in the ground state of the bottom QD. The ground state for a hole in the bottom QD is a metastable state in the sense that the hole can relax to the ground state of the top QD, which is at lower energy. The presence of the AlGaAs barrier is expected to slow hole relaxation from the bottom QD to the top QD, and thus it is not too surprising that this QDM structure increases the probability of observing an extra hole trapped in the bottom QD. However, we do not observe the "echo" PL lines for all ranges of electric fields or for all the assigned PL lines. We present a model that explains how competing charge relaxation
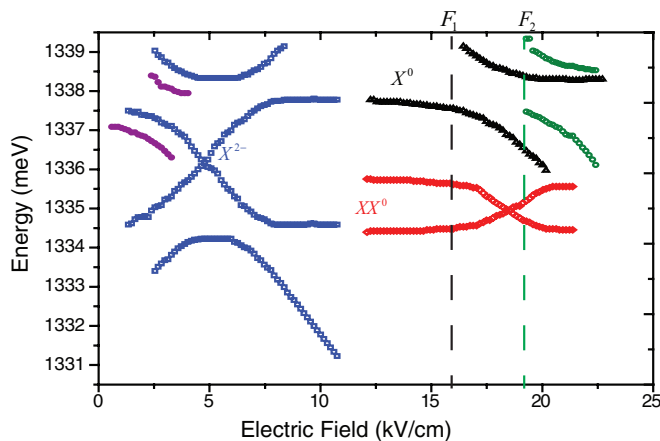

FIG. 2. (Color online) Energy of emitted PL as a function of electric field. Symbols indicate different charge states: neutral exciton state (X^0, black triangles), biexciton (XX^0, red diamonds), doubly negatively charged trion (X^{2-}, blue squares). Open green circles and solid purple circles originate from charge states with a dynamically trapped hole in the bottom QD.

and tunneling dynamics permit a single hole to be trapped in this metastable state. We show that this model explains why the PL "echoes" occur only for certain ranges of applied electric field. We further validate the model with measurements of the emitted PL as a function of electric field.

In the following discussion of we use $\binom{e_B e_T}{h_B h_T}$ to describe the spatial location of charges in the QDM. e_B (e_T) are the number of electrons in the bottom (top) QD; h_B (h_T) are the corresponding number of holes. This notation describes the atomiclike states of the QDM when energy levels are not in resonance and charges are localized to individual QDs. When the electric field tunes energy levels into resonance, coherent tunneling leads to the formation of anticrossings and the molecular states can be described as symmetric and antisymmetric combinations of these basis states. We use underlines to indicate the charge carriers participating in optical recombination and photon emission. For example, $\binom{11}{0\underline{2}}$ is the optical emission from the XX^0 state with one electron in each QD and both holes in the top QD. The emitted photon comes from the radiative recombination of an electron and hole in the top QD.

A. Dynamic hole trapping in the X^0 state

The X^0 (neutral exciton) state contains one electron and one hole generated by nonresonant excitation. If the electron and hole both relax into the top QD we get optical emission from the $\binom{01}{0\underline{1}}$ state. This process is schematically depicted by path 1a in Fig. 3. If the electron relaxes to the bottom QD and the hole relaxes to the top QD (path 1b in Fig. 3) we get optical emission from the $\binom{10}{0\underline{1}}$ state. Coherent tunneling between these two states when the electron energy levels are in resonance leads to the anticrossing of the black triangles as

FIG. 3. (Color online) Kinetic pathways that results in optical emission from X^0 states with and without dynamically trapped holes.

shown in Fig. 2. In both of these cases the hole relaxes to the top QD. The relaxation of the hole to the top QD can occur either by localization to excited states of the top QD before relaxation to the QD ground states or by relaxation to the ground state of the bottom QD followed by phonon assisted tunneling through the barrier to the lower energy hole state localized in the top QD. If the hole and electron both localize in the bottom QD we get optical emission from the $\binom{10}{\underline{1}0}$ state. Because the bottom QD is truncated to 2.6 nm, PL emission from the bottom QD would be outside the energy range plotted in Fig. 2. We do not typically observe PL emission at higher energies that could be assigned to the $\binom{10}{\underline{1}0}$ state.

The green circles in Fig. 2 echo the anticrossing of the X^0 state, but the anticrossing is shifted by 3.15 kV/cm from F_1 to F_2. We assign the "echo" PL emission to the presence of one additional hole in the bottom QD. The kinetic pathways that lead to the formation of this state are shown in path 2 of Fig. 3. The additional hole is created by optical charging: an optically generated electron and hole relax into the bottom QD, but the electron tunnels out of the QDM leaving the hole behind. The presence of the AlGaAs barrier slows the hole relaxation to the top QD and makes it possible for a second optically generated electron-hole pair to relax to the ground states of the top QD and recombine, resulting in emission from the $\binom{01}{1\underline{1}}$ state [Fig. 3 (2)]. A similar path leads to the emission from the $\binom{10}{1\underline{1}}$ state. Coherent tunneling of the electron between these two states results in the anticrossing of the green circles in Fig. 2. The electric field at which this anticrossing occurs (F_2) is shifted relative to the X^0 case (black triangles, anticrossing at F_1) because the Coulomb interactions with the additional hole in the bottom QD shift the confined energy levels.

Optical emission from the $\binom{01}{1\underline{1}}$ and $\binom{10}{1\underline{1}}$ states is only observed under relatively high values of the net electric field in the sample ($18 \leqslant F \leqslant 20$ kV/cm). PL emission from these states disappears as the electric field decreases because the probability for the electron to escape from the bottom QD decreases with electric field. In Fig. 4 we plot the lifetime of electrons in the bottom QD as a function of electric field (solid line). This lifetime is calculated from the inverse of the rate of electron escape via Fowler-Nordheim tunneling through the
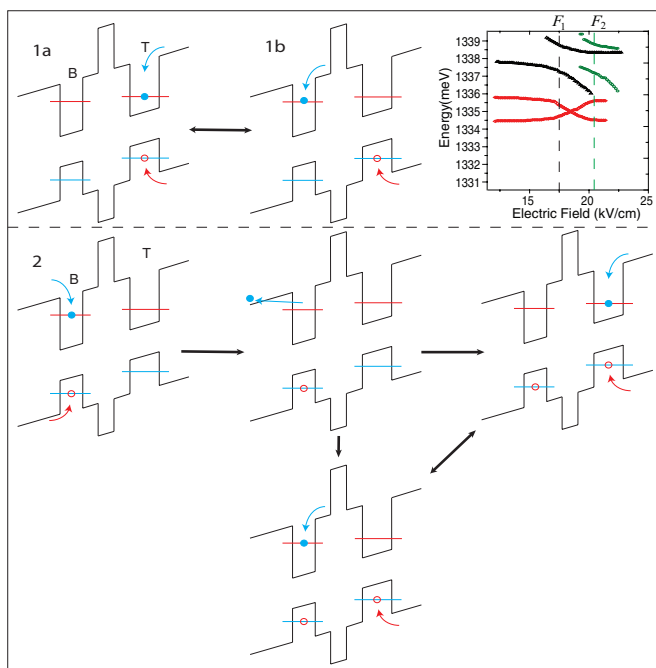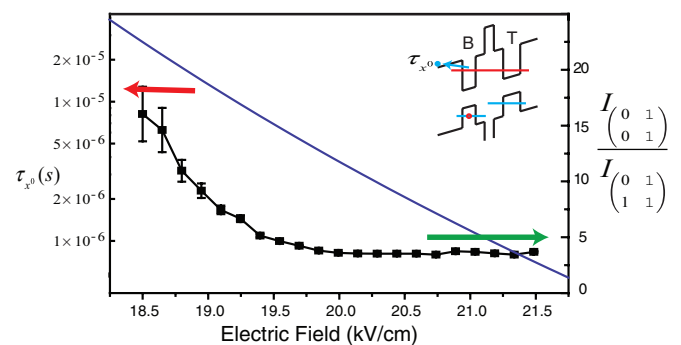

FIG. 4. (Color online) Left: Lifetime of the electron in the bottom dot as the function of electric field. Right: Ratio of intensity of PL emission from states without and with the presence of a dynamically trapped hole.

triangular barrier using

$$\tau_{x^0} = \frac{\sqrt{E_0}}{(\sqrt{2 * m_{\text{GaAs}}} * l)} \exp\left(\frac{4\sqrt{2 * m_{\text{GaAs}} * W^3}}{(3 * e * \hbar)}\right), \quad (1)$$

where E_0 is the confined state energy; m_{GaAs} is the effective mass of electrons in GaAs barrier; W is the energy gap between the GaAs conduction-band edge and E_0. The lifetime calculated by Eq. (1) decreases as the electric field increases because the triangular tunnel barrier bounding the bottom edge of the bottom QD becomes thinner. The calculations reveal that the electron lifetime increases by more than one order of magnitude as the electric field decreases from 22 to 18 kV/cm.

In Fig. 4 we also compare the calculated lifetime of the electron in the bottom QD to the probability of observing a dynamically trapped hole. We quantify the probability of having a state with a dynamically trapped hole by analyzing the ratio of PL intensity from X^0 states with and without a dynamically trapped hole as a function of electric field. The intensity of PL emission from the X^0 states with a dynamically trapped hole is labeled $I\left(\begin{smallmatrix}01\\1\bar{1}\end{smallmatrix}\right)$; the intensity of PL emission from the X^0 states without a dynamically trapped hole is labeled $I\left(\begin{smallmatrix}01\\0\bar{1}\end{smallmatrix}\right)$. The PL intensity ratio $I\left(\begin{smallmatrix}01\\0\bar{1}\end{smallmatrix}\right)/I\left(\begin{smallmatrix}01\\1\bar{1}\end{smallmatrix}\right)$ decreases with increasing electric field because the probability of electron escape from the bottom QD increases. As the lifetime of the electron in the bottom QD increases, with decreasing electric field, it becomes increasingly likely that electrons and holes will recombine in the bottom QD. Consequently, for electric fields below about 18 kV/cm we do not observe PL emitted by X^0 states in the presence of a dynamically trapped hole.

The ratio of the PL intensity from states without and with a dynamically trapped hole falls more rapidly than the calculated electron lifetime. We believe this is due to the fact that the hole can remain trapped in the bottom QD for many optical excitation cycles. Once the electron has escaped the bottom QD, all subsequent optical emission events involving an electron and hole in the top QD will be perturbed by the presence of the hole trapped in the bottom QD [i.e., $\left(\begin{smallmatrix}01\\1\bar{1}\end{smallmatrix}\right)$ or $\left(\begin{smallmatrix}10\\1\bar{1}\end{smallmatrix}\right)$]. Emission only from states that involve a dynamically trapped hole will persist until the hole escapes, which is much slower than the escape of the electron due to the higher hole effective mass.

B. Dynamic hole trapping in the X^{2-} state

For the doubly negatively charged trion (X^{2-}), the two excess electrons tunnel into the QDM from the n-doped substrate. This occurs at low values of the net electric field, when the confined states of the QDs cross the Fermi level set by the doping. The two electrons can be in the same QD or in separate QDs. The excess hole responsible for the PL echo lines (solid purple circles) observed between 0.34 and 4.15 kV/cm is again formed by optical charging: an electron and hole are optically generated in the bottom QD by the exciting laser, but the electron tunnels out of the QDM and leaves the hole behind. Following the analysis in Sec. III A, we know that the probability that the electron tunnels out of the ground state of the bottom QD is negligibly small at low values of the net electric field. As described in Fig. 6, the electron can be trapped in an excited
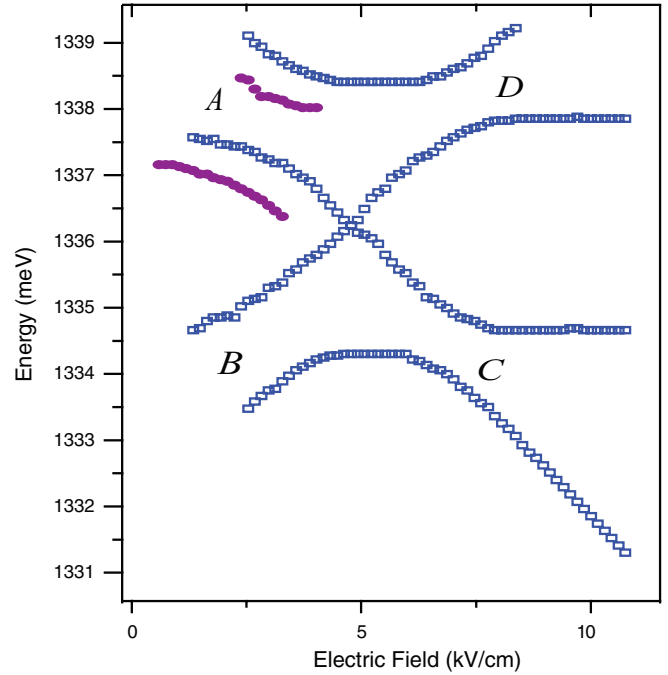

FIG. 5. (Color online) The x pattern for the X^{2-} state.

state of the bottom QD due to the presence of two electrons occupying the ground state of the bottom QD. The lifetime of the electron in this excited state is significantly shorter than in the ground state, allowing the escape of the electron and the optical charging of the bottom QD with a hole. As we now show, analysis of the dynamic pathways that lead to trapping of an excess hole in the X^{2-} state explain why the "echo" lines appear for only a subset of the X^{2-} "x" pattern.

We consider first the portion of the X^{2-} "x" pattern where the PL "echo" lines appear (anticrossing A in Fig. 5). The dynamic pathways that result in typical emission of the X^{2-} state (i.e., without an extra spectator hole) are described in Fig. 6 (A1): two electrons occupy the ground state of the bottom QD and an optically generated electron and hole relax into the ground state of the top QD, resulting in emission from the $\left(\begin{smallmatrix}21\\0\bar{1}\end{smallmatrix}\right)$ state. If the optically generated electron and hole relax into the bottom QD, as shown in Fig. 6 (A2), the electron cannot relax to the QD ground state, which is fully occupied by two electrons. As a result, the electron is trapped in a higher energy state from which it can tunnel out to the doped substrate. Calculations of the electron lifetime in the excited state of the bottom QD, using an equation analogous to Eq. (1), indicate that the electron lifetime in the excited state is of order 10^{-9} s even for relatively low values of the net electric field.

We turn next to anticrossing B and C of Fig. 5. To observe optical emission in these regions, the two electrons present in the QDM before optical excitation must be located in separate QDs [i.e., $\left(\begin{smallmatrix}11\\00\end{smallmatrix}\right)$]. If the optically generated electron and hole relax into the top QD, they can recombine in emission from the $\left(\begin{smallmatrix}12\\0\bar{1}\end{smallmatrix}\right)$ state, which has PL energy similar to the X^- state (i.e., redshifted relative to the X^0 by 3–6 meV). This pathway is shown in Fig. 6 (B1). If the optically generated electron
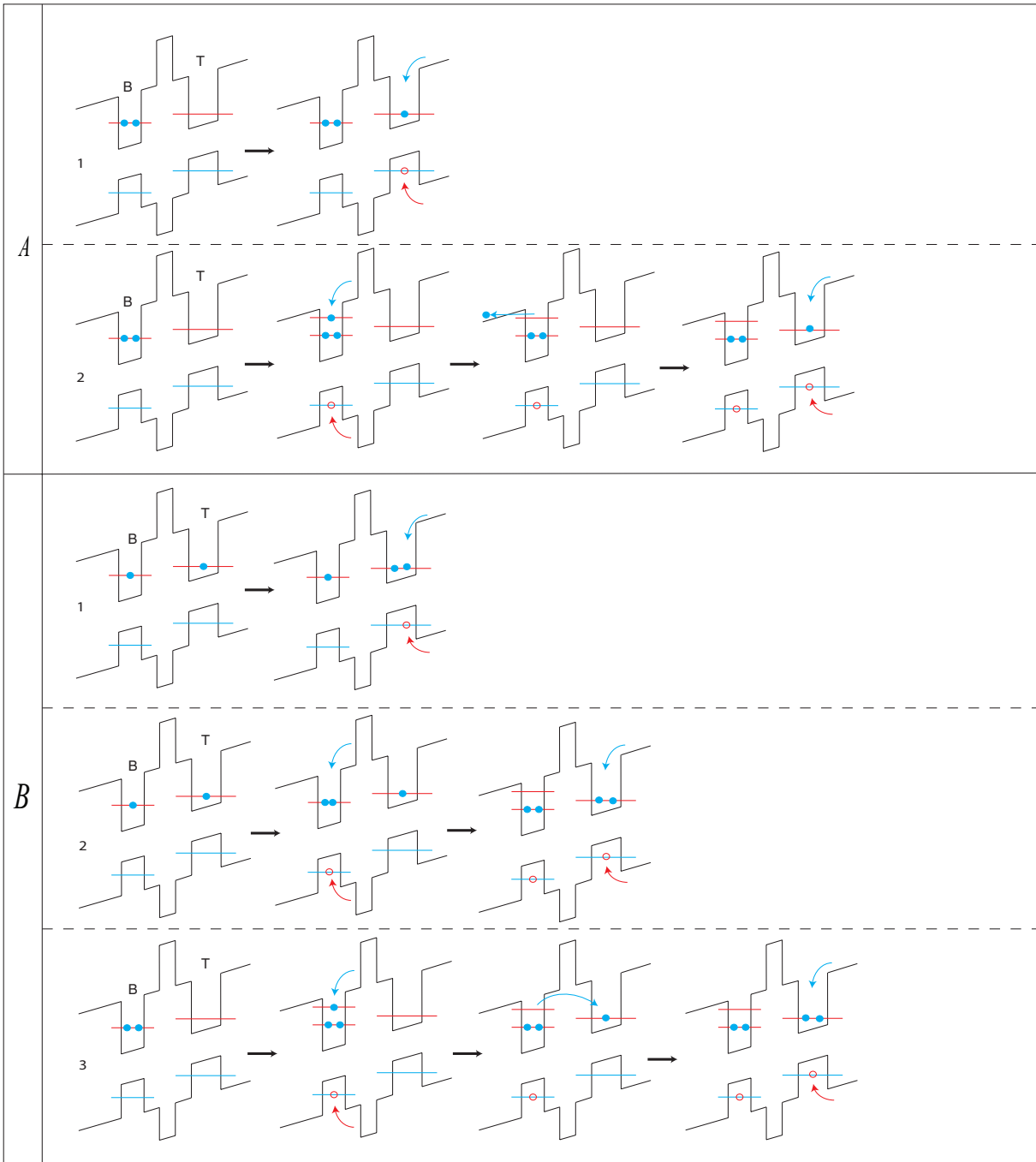
FIG. 6. (Color online) Dynamic pathways to create different spatial configurations of the X^{2-} state with and without the extra dynamic trapped hole.

and hole relax into the bottom QD the electron can relax all the way to the ground state, and therefore does not escape the bottom QD. Subsequent capture of an optically generated electron and hole in the top QD results in emission from an X^{3-} state, as depicted in Fig. 6 (B2). The Coulomb interactions with the additional electron shift the energy of the PL emission of this X^{3-} state relative to the X^{2-} state and no PL "echo" is observed. We note that tunneling of an electron from the excited state of the bottom QD into the top QD, as depicted in Fig. 6 (B3), similarly results in emission from an X^{3-} state and the absence of a PL echo. However, the emission from the

X^{3-} state will be in a drastically different energy region due to the Coulomb shift, therefore we cannot include this state in the energy region we shown for X^{2-} here.

For anticrossing D, the kinetic pathway is similar to anticrossing A, but the anticrossing is formed by the tunnel coupling of $\binom{20}{00}$ and $\binom{11}{00}$ in the initial state before optical excitation. Because the initial state contains a significant contribution from $\binom{11}{00}$, the electron relaxation to the ground state is not effectively blocked and the dynamic hole trapping effect is not observed.
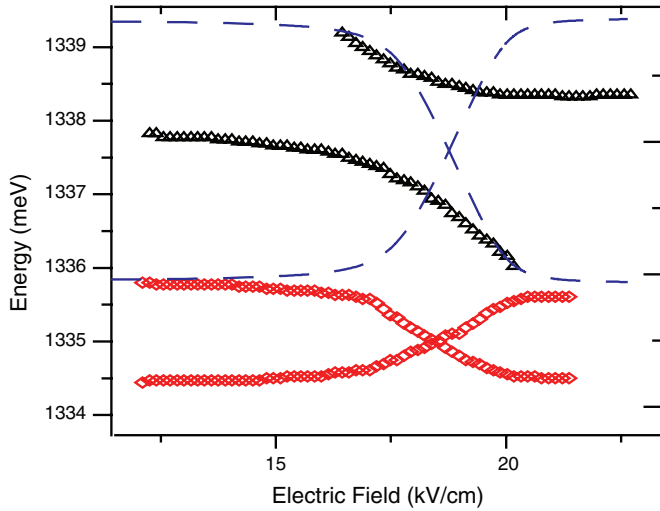
FIG. 7. (Color online) PL for biexciton states. Blue dashed lines are simulation of the commonly observed biexciton PL from a typical InAs/GaAs QDM.

C. Dynamic hole trapping in the XX^0 state

In previously investigated QDMs designed for electron tunneling, holes rapidly relax to a single QD (e.g., the top QD). The commonly observed biexciton (XX^0) PL emission originates in two spatial configurations of charges: $\binom{11}{02}$ and $\binom{02}{02}$. The first of these charge configurations results in PL emission with energy similar to that of a positive trion, typically blueshifted by about 1 meV relative to the X^0 in QDMs we have previously investigated. The second of these charge configurations results in PL emission with energy similar to the biexciton state of a single QD, redshifted relative to the X^0 by approximately 2 meV. Coherent tunneling of an electron between these charge states leads to the formation of an "x" pattern. The solid gray lines in Fig. 7 schematically indicate the approximate energy, relative to the observed X^0 PL, at which we would expect to observe PL emission from a typical XX^0 x pattern. It is clear that the experimentally observed PL, indicated by the red diamonds, does not follow this form. We have not observed typical XX^0 PL x patterns in any of the six QDMs containing AlGaAs barriers that we have investigated. We confirm that the observed PL lines originate in biexcitonic states by measuring the intensity of these lines, relative to the X^0 PL, as a function of excitation laser intensity (data not shown).

We now show that the biexciton pattern we observe originates in the presence of a single excess hole dynamically trapped in the bottom QD. One of the observed XX^0 PL lines is redshifted relative to the X^0 PL by approximately 3 meV, similar to the redshift observed for the X^--like charge configuration of the X^{2-} state. We therefore postulate that the XX^0 PL line redshifted by 3 meV relative to the X^0 is attributed to $\binom{02}{1\underline{1}}$.

The presence of the AlGaAs barrier is expected to suppress hole tunneling, so that the $\left(\binom{02}{11}\right)$ charge configuration is more probable in this QDM design than in regular designs with only GaAs barriers. The fact that we do not observe PL emission that can be attributed to $\binom{11}{02}$, but do observe PL emission from $\binom{02}{1\underline{1}}$, suggests that the addition of Al to the barrier suppresses a typical pathway for the formation of the $\binom{11}{02}$ XX^0 state. The results therefore suggest that the typical pathway for formation of the $\binom{11}{02}$ state involves localization of two optically generated holes in separate QDs, followed by phonon-assisted hole tunneling through the barrier that allows the hole from the higher energy QD to reach the ground state of the low-energy QD. The addition of Al to the barrier in these QDMs suppresses that hole tunneling and leads to the absence of $\binom{11}{02}$ PL and the appearance of $\binom{02}{11}$ PL associated with a dynamically trapped hole.

IV. CONCLUSION

We present photoluminescence spectroscopy measurements of a single QDM consisting of InAs QDs separated by a barrier that contains AlGaAs. The observed PL contains several photoluminescence lines that cannot be explained by existing models in which holes rapidly relax to the lowest energy state in the top QD. We show that all of these lines can be explained by the presence of a hole trapped in the ground state of the bottom QD, a metastable state at higher energy than the ground state of the top QD. We present a model of the charge relaxation dynamics that lead to the population of this metastable state under certain conditions. The results provide insight into both the charge relaxation dynamics in coupled QDs and the magnitude of Coulomb interactions between charges trapped in closely spaced QDs.

*doty@udel.edu

[1] F. H. L. Koppens, J. A. Folk, J. M. Elzerman, R. Hanson, L. H. W. van Beveren, I. T. Vink, H. P. Tranitz, W. Wegscheider, L. P. Kouwenhoven, and L. M. K. Vandersypen, Science **309**, 1346 (2005).

[2] D. Loss and D. P. DiVincenzo, Phys. Rev. A **57**, 120 (1998).

[3] A. Shields, Nat. Photon. **1**, 215 (2007).

[4] M. F. Doty, J. I. Climente, M. Korkusinski, M. Scheibner, A. S. Bracker, P. Hawrylak, and D. Gammon, Phys. Rev. Lett. **102**, 047401 (2009).

[5] W. Liu, S. Sanwlani, R. Hazbun, J. Kolodzey, A. S. Bracker, D. Gammon, and M. F. Doty, Phys. Rev. B **84**, 121304 (2011).

[6] M. Bayer, G. Ortner, O. Stern, A. Kuther, A. A. Gorbunov, A. Forchel, P. Hawrylak, S. Fafard, K. Hinzer, T. L. Reinecke *et al.*, Phys. Rev. B **65**, 195315 (2002).

[7] D. Gammon, E. S. Snow, B. V. Shanabrook, D. S. Katzer, and D. Park, Phys. Rev. Lett. **76**, 3005 (1996).

[8] V. D. Kulakovskii, G. Bacher, R. Weigand, T. Kümmell, A. Forchel, E. Borovitskaya, K. Leonardi, and D. Hommel, Phys. Rev. Lett. **82**, 1780 (1999).

[9] L. Landin, M. S. Miller, M. E. Pistol, C. E. Pryor, and L. Samuelson, Science **280**, 262 (1998).

[10] H. J. Krenner, M. Sabathil, E. C. Clark, A. Kress, D. Schuh, M. Bichler, G. Abstreiter, and J. J. Finley, Phys. Rev. Lett. **94**, 057402 (2005).

[11] M. F. Doty, M. Scheibner, A. S. Bracker, I. V. Ponomarev, T. L. Reinecke, and D. Gammon, Phys. Rev. B **78**, 115316 (2008).

[12] E. A. Stinaff, M. Scheibner, A. S. Bracker, I. V. Ponomarev, V. L. Korenev, M. E. Ware, M. F. Doty, T. L. Reinecke, and D. Gammon, Science **311**, 636 (2006).

[13] H. J. Krenner, E. C. Clark, T. Nakaoka, M. Bichler, C. Scheurer, G. Abstreiter, and J. J. Finley, Phys. Rev. Lett. **97**, 076403 (2006).

[14] M. F. Doty, M. Scheibner, A. S. Bracker, and D. Gammon, in *Single Semiconductor Quantum Dots*, edited by P. Michler (Springer, Berlin, 2009), pp. 331–366.

[15] M. F. Doty, M. Scheibner, I. V. Ponomarev, E. A. Stinaff, A. S. Bracker, V. L. Korenev, T. L. Reinecke, and D. Gammon, Phys. Rev. Lett. **97**, 197202 (2006).

[16] M. Scheibner, M. Doty, I. Ponomarev, A. Bracker, E. Stinaff, V. Korenev, T. Reinecke, and D. Gammon, Phys. Rev. B **75**, 245318 (2007).

[17] A. S. Bracker, M. Scheibner, M. F. Doty, E. A. Stinaff, I. V. Ponomarev, J. C. Kim, L. J. Whitman, T. L. Reinecke, and D. Gammon, Appl. Phys. Lett. **89**, 233110 (2006).

[18] D. Kim, S. E. Economou, S. C. Badescu, M. Scheibner, A. S. Bracker, M. Bashkansky, T. L. Reinecke, and D. Gammon, Phys. Rev. Lett. **101**, 236804 (2008).

[19] S. A. Wolf, D. D. Awschalom, R. A. Buhrman, J. M. Daughton, S. von Molnar, M. L. Roukes, A. Y. Chtchelkanova, and D. M. Treger, Science **294**, 1488 (2001).

[20] A. Imamoglu, D. D. Awschalom, G. Burkard, D. P. DiVincenzo, D. Loss, M. S. Sherwin, and A. Small, Phys. Rev. Lett. **83**, 4204 (1999).

[21] A. Imamoglu, E. Knill, L. Tian, and P. Zoller, Phys. Rev. Lett. **91**, 017402 (2003).